

# Characterization of magneto-optical recording media in terms of domain boundary jaggedness

Cite as: Journal of Applied Physics **69**, 4960 (1991); <https://doi.org/10.1063/1.348188>  
Published Online: 17 August 1998

Bruce E. Bernacki, and M. Mansuripur



View Online



Export Citation

## Ultra High Performance SDD Detectors



See all our XRF Solutions

# Characterization of magneto-optical recording media in terms of domain boundary jaggedness

Bruce E. Bernacki and M. Mansuripur  
*Optical Sciences Center, University of Arizona, Tucson, Arizona 85721*

Noise in magneto-optical recording devices can be classified as system-related noise and media noise. Media noise is rooted in the magnetic and magneto-optical properties of the recording media. To investigate media noise and its relation to microstructure and micromagnetics of thin films, the jaggedness of magnetic domain boundaries is characterized using static domain observations in which the fractal dimension  $D$  is measured for the domain boundaries. Samples of TbFeCo deposited under similar conditions, but with slightly different compositions, exhibited different amounts of jaggedness, and hence, slightly different values of  $D$ , i.e.,  $1.05 < D < 1.20$ . Temperature dependent measurements performed on a TbFe sample showed increasing  $D$  with increasing temperature,  $1.19 < D < 1.28$  for  $300 \text{ K} < T < 360 \text{ K}$ . Possible sources of jaggedness include structural/magnetic inhomogeneities as well as competition between domain-wall energy and demagnetization.

## I. INTRODUCTION

Noise in magneto-optical (MO) recording devices can be classified into five distinct categories: (i) electronic noise, (ii) shot noise, (iii) laser noise, (iv) erased media noise, and (v) domain boundary noise. The first three classes are system-related noises, whereas the last two are rooted in the magnetic and magneto-optical properties of the recording media. The ultimate signal-to-noise ratio (SNR) presently attainable in MO storage systems is limited by media noise. Erased media noise is due to spatial variations of structural/magnetic properties of the media. Such variations manifest themselves in the domain structures that are grown slowly, to allow domain walls to follow the terrain with little assistance from the outside. Thus, measurements of the degree of jaggedness of such domains can be used to characterize the degree of nonuniformity of the media. Since it has been shown that an increase in domain-wall irregularity results in decreased carrier-to-noise ratio (CNR) of the recording system,<sup>1</sup> measuring domain-wall jaggedness may shed light on the character of noise in MO media. At present, a satisfying method for quantifying domain-wall shape does not exist. Clearly, a single figure of merit for domain-wall shape would provide a quantitative measure of the SNR potential of MO materials very early in the development process, and would permit easy comparison between different materials. The measured fractal dimension  $D$  of the magnetic domain wall can provide this figure of merit.

## II. BACKGROUND

A fractal curve is nonrectifiable and thus cannot be described using Euclidean geometry. More formally, a fractal structure is one whose Hausdorff-Besicovitch dimension  $D$  exceeds its topological dimension  $D_T$ .<sup>2</sup> For a one-dimensional profile, such as a domain wall,  $1 < D < 2$ , with  $D=1$  corresponding to a one-dimensional Euclidean curve, and  $D=2$  corresponding to a plane-filling curve.

Fractals exhibit the property of scaling, which is further divided into the properties of self-similarity and self-

affinity.<sup>2</sup> Strict self-similarity is seldom encountered in nature, so one resorts to a statistical form of self-similarity to describe natural objects. Statistical self-similarity means that each portion of an object can, in a statistical sense, be regarded as a reduced-scale version of the entire object. Self-affinity is a more restrictive form of scaling in which there is a non-linear mapping between the original function and its scaled version.<sup>2,3</sup>

An elegant technique to measure fractal dimension was first suggested by Richardson<sup>4</sup> in his measurement of the length of the coastline of Britain, and is termed the compass dimension<sup>5</sup> or ruler method. In this method, rulers with different lengths  $\epsilon$  are used to measure the length  $L(\epsilon)$  of a boundary. The length  $L(\epsilon)$  is the product of the number of rulers needed to span the boundary and the ruler length  $\epsilon$ . If the total length  $L(\epsilon)$  of the boundary is plotted versus the ruler length  $\epsilon$  on a log-log scale for a fractal profile, the points will lie on a straight line as follows<sup>5</sup>:

$$\log[L(\epsilon)] = (1 - D)\log(\epsilon) + \log(C),$$

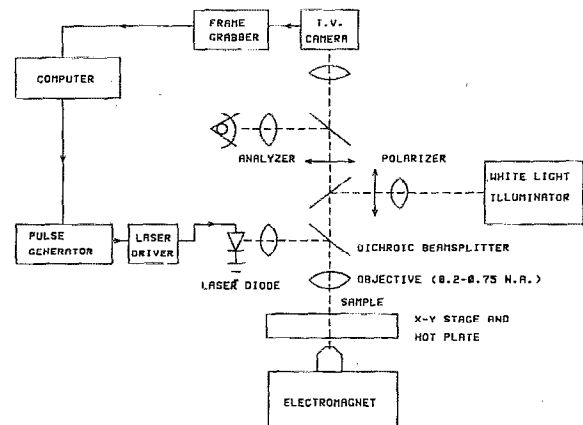


FIG. 1. Experimental setup for measuring fractal dimension of MO domains.

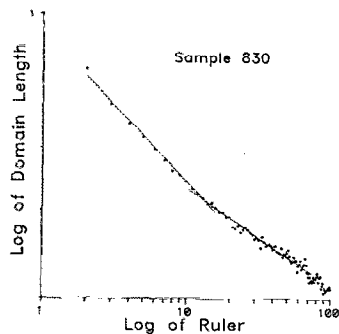


FIG. 2. Graph of  $L(\epsilon)$  vs  $\epsilon$  for  $1 \leq \epsilon < 100$  units. Note the two distinct bands with different slopes between the inner and outer ruler length cutoffs.

where  $C$  is a constant.

Natural objects are not mathematical constructs, and are not statistically self-similar or self-affine over all ranges of ruler lengths, but only over a limited band of ruler lengths that must be determined experimentally. This is determined in the present work by analyzing the log-log plot of the total length of the digitized profile versus ruler length for a range of ruler lengths. In general, all of the points will not lie on a single straight line, but bands of data points will lie on lines of different slopes between two breakpoints called the inner cutoff and outer cutoff.<sup>2</sup> Following the method of Burrough,<sup>6</sup> the line of maximum slope between the inner and outer cutoff was chosen for this study to measure  $D$ , since when the sampling interval matches the scale of the phenomenon present in the object under study, a lower measure of  $D$  than is expected results. Hence, the line with the greatest slope gives the more accurate measure.

### III. EXPERIMENTAL SETUP

The MO domains are recorded and observed using the experimental setup shown in Fig. 1. The heart of the system is a polarized-light microscope, which has been modified for thermomagnetic recording by the addition of a laser diode and bias magnet, as well as a thermal stage for temperature-dependent studies. An RS-170 video camera is used to image the domains, with single frame storage provided by a personal computer-based frame grabber.

Data is acquired by thermomagnetically writing a micrometer-sized reverse-magnetized domain with a small bias field ( $\approx 300$  Oe), and up to 12 mW of laser power. The bias field is then slowly increased to expand the domain until the domain wall is approximately 50 pixels in diameter to ensure adequate sampling of the image. Alter-

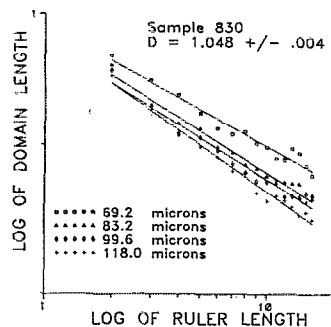


FIG. 3. Graph of  $L(\epsilon)$  vs  $\epsilon$  for the first band of ruler lengths shown in Fig. 2. Different symbols (each with least-squares-fitted line) correspond to different expansions of domains. Domain diameters given in the legend. Fractal dimension  $D$  is  $1 - m$ , where  $m$  is the slope for each line.  $D$  given is the average of the four values, along with calculated standard deviation.

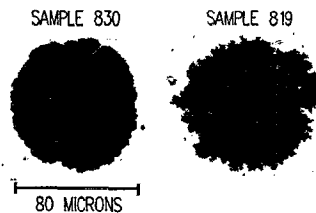


FIG. 4. Comparison of two markedly different MO films. Image at left shows domain in a  $\text{Tb}_{17.2}\text{Fe}_{60.3}\text{Co}_{7.4}\text{Ar}_{15.4}$  film (sample 830). The domain on the right was recorded on a  $\text{Tb}_{22.9}\text{Fe}_{58.4}\text{Co}_{9.4}\text{Ar}_{9.3}$  film (sample 819).

natively, a line can be written across the MO material by advancing the microscope stage in a fixed direction while the laser is pulsed rapidly. The line domain is then expanded in the same manner as the circular domain. The image is then digitized and frame averaged for noise reduction, and the image is made binary using standard video microscopy techniques.

Image processing software is used to extract the boundary of the domain. At this point, rulers of different length  $\epsilon$  are translated along the boundary of the domain, and the number of rulers needed to span the boundary  $N$  is recorded for  $1 \leq \epsilon < 100$  pixels. Remainder distances at the end of the domain boundary are added to the ruler count as fractions of a ruler length for each different ruler size. One need not be concerned with the choice of starting point as long as the ruler length  $\epsilon$  is short enough,<sup>5</sup> as it is in all cases considered here. A log-log plot is made of the boundary length  $L(\epsilon)$  versus ruler length  $\epsilon$ , and the appropriate band of ruler lengths is determined for calculation of  $D$ . Figure 2 shows such a plot with two distinct bands. The band exhibiting the greatest slope between the inner and outer cutoff is selected as the measure of  $D$  for the boundary. The fractal dimension is related to the slope  $m$  of the fitted line by the equation

$$D = 1 - m,$$

where  $m$  is generally a small negative number. Figure 3 shows the final log-log plot of  $L(\epsilon)$  vs  $\epsilon$  for several domain expansions of a  $\text{Tb}_{17.2}\text{Fe}_{60.3}\text{Co}_{7.4}\text{Ar}_{15.2}$  sample (sample 830).

### IV. EXPERIMENTAL RESULTS

The measurements taken to date are repeatable, and show good correlation between qualitative evaluation of domain-wall irregularity and the measured fractal dimension  $D$ . That is, as the amount of domain-wall jaggedness appears to increase visually,  $D$  increases. Figure 4 shows the contrast between domains in two TbFeCo films (sample 830 and 819, which has composition  $\text{Tb}_{22.9}\text{Fe}_{58.4}\text{Co}_{9.4}\text{Ar}_{9.3}$ ) that exhibit markedly different degrees of domain-wall jaggedness. Domains were written in each sample and then expanded to 60  $\mu\text{m}$  in diameter, as described earlier. The ruler technique was applied to the

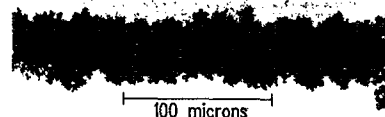


FIG. 5. A line domain written in sample 819.

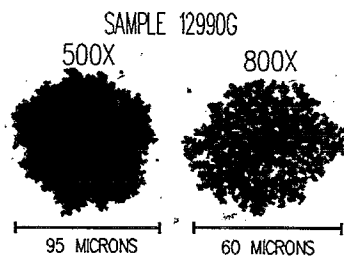


FIG. 6. The images are of two different domains written in the  $Tb_{18.3}Fe_{74.5}Ar_{7.2}$  film (sample 12990G) and imaged at different magnifications: (a) 95  $\mu m$  diameter, imaged at 500 $\times$ ; (b) 60  $\mu m$  diameter, imaged at 800 $\times$ .

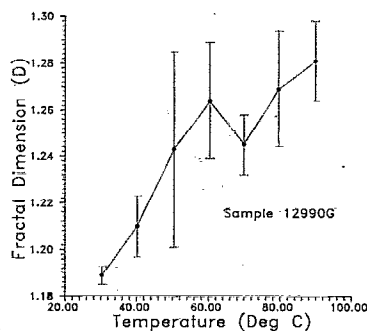


FIG. 7. Plot of fractal dimension  $D$  for domains written and expanded at various ambient temperatures. Error bars represent the standard deviation of the measured  $D$ .

original and three additional expansions, up to a diameter of 130  $\mu m$ . After selecting the appropriate band of data points, the measure of  $D$  was determined for each expansion. These measurements were averaged, and their standard deviations calculated. The measurement of  $D$  that resulted for sample 819 for four expansions (62.8–118.0  $\mu m$ ) was  $1.208 \pm 0.019$ , significantly larger than the figure of  $1.048 \pm 0.004$  for the value of  $D$  of sample 830.

Either line or circular domains can be written and measured. An example of a line domain written in sample 819 is shown in Fig. 5. The measure of  $D$  for the line domain for four expansions (20.0–55.6  $\mu m$ ) was found to be  $1.189 \pm 0.010$ , which is within one standard deviation of measurement for a circular domain in sample 819.

Since natural objects are generally not perfectly scaling, the measurement of  $D$  for most natural objects will depend on the band of ruler lengths over which the measurement is made, and in some cases, the magnification at which the measurement is made. The latter case is true of MO domains, since, in general,  $D$  increases when the magnification of the image is increased. Figures 6(a) and 6(b) are images of domains in the same  $Tb_{18.3}Fe_{74.5}Ar_{7.2}$  film (sample 12990G) imaged at 500 $\times$  and 800 $\times$ , respectively. In Fig. 6(b), the apparent increase in jaggedness with increased magnification is clearly evident when compared with Fig. 6(a). This limits the application of the proposed technique to measurements taken at the same magnification if comparisons are to be made between different materials, and implies that a different technique may be more appropriate to measure the fractal dimension.<sup>7</sup> A measurement series for four expansions (60–95  $\mu m$ ) for this sample at 500 $\times$  resulted in a value for  $D$  of  $1.175 \pm 0.012$ . At 800 $\times$ , a four-expansion sequence in this same material (40–90  $\mu m$ ) gave a measure of  $D$  of  $1.259 \pm 0.029$ .

Measurements were also made to determine the jaggedness for the domain walls written and expanded at elevated temperatures, beginning at 300 K. Domains were written and expanded four times in 10-K steps, from 300 to 360 K. For sample 12990G, the average  $D$  and corresponding standard deviation is plotted versus temperature in Fig.

7. The value of  $D$  increases as the sample temperature approaches the Curie temperature  $T_c$  (approximately 390 K for this sample). Possible causes for this increase in  $D$  are currently under investigation.

## V. CONCLUSION

State-of-the-art MO recording systems are presently limited by media noise, which is contributed to by structural/magnetic inhomogeneities and by the irregularities in the recorded domain walls. Until now, a simple way to categorize and describe domain-wall irregularity did not exist. The measured fractal dimension  $D$  can provide a unique, relatively easy-to-measure figure of merit for determining the degree of domain-wall jaggedness. Although it appears that MO domains are self-affine, so long as the measurements are made at the same magnification, distinct and repeatable values of the fractal dimension  $D$  can be obtained for each material of interest. This technique provides a new tool for the MO materials researcher to use in evaluating potential MO recording films.

## ACKNOWLEDGMENTS

The authors gratefully acknowledge the support of Optical Data Storage Center at the University of Arizona for this work. Some of the samples were prepared by Dr. David Shieh of the IBM Corporation. Mr. Roger Hajjar did bulk magnetic and magneto-optic measurements on the samples reported in this paper.

<sup>1</sup>C.-J. Lin, MRS Symp. Proc. **150**, 15 (1989).

<sup>2</sup>B. B. Mandelbrot, *The Fractal Geometry of Nature* (W. H. Freeman, New York, 1983).

<sup>3</sup>Scaling is self-affine if there exists an exponent  $\alpha > 0$  such that for every  $h > 0$ ,  $L(\epsilon)$  is statistically identical to  $h^{-\alpha}L(h\epsilon)$ . This requires that one check all mathematical possibilities of  $L(\epsilon)$  and  $h^{-\alpha}L(h\epsilon)$ , and this can never be proved for practical cases.

<sup>4</sup>L. F. Richardson, *General Systems Yearbook* **6**, 139 (1961).

<sup>5</sup>B. Mandelbrot, *Science* **156**, 637 (1967).

<sup>6</sup>P. A. Burrough, *Nature* **294**, 240 (1981).

<sup>7</sup>B. B. Mandelbrot, *Phys. Scr.* **32**, 257 (1985).